

ION BEAM EXTRACTION FROM MAGNETIZED PLASMA

P. Spadtke, K. Tinschert, R. Lang, J. Mader, F. Maimone, J. Roßbach, GSI Darmstadt

Abstract

By increasing the total extracted ion current, the optimization of the extraction system becomes more important for any ion source because of the space charge effect. Several attempts have been made in the past to simulate the extraction from an Electron Cyclotron Resonance Ion Source (ECRIS) in a correct way. Most of these attempts failed, because they were not able to reproduce the experimental results. The best model up to now is given by the following procedure:

- Tracing the magnetic field lines through the extraction aperture, looking where these field lines are coming from.
- Using these coordinates of the magnetic field line as starting points for ions to be extracted.
- The initial current of each trajectory is determined by theoretical assumptions about the plasma or by a plasma simulation.
- Childs law is applicable locally only in direction of the magnetic field, if no emission limited flow is present.

INTRODUCTION

This model assumes that ions travel through the plasma only influenced by the magnetic field. The positive ions inside the plasma chamber are assumed to be space charge compensated to a very high degree because of the presence of cold electrons, resulting in a small plasma potential. Collisions are neglected for the path of the ion, as well as diffusion effects inside the plasma. The radius of gyration for cold electrons is well within the μm range, and so the radius of gyration for ions is below the mm range. This is a necessary precondition to define the ECRIS plasma to be magnetized. The assumption that diffusion processes are playing also a minor role is supported by the experimental experience that plasma etching occurs only at places in the plasma chamber pronounced by the magnetic structure. The visible traces inside the plasma chamber and on both end plates of the plasma chamber (injection side plate and plasma electrode) are sharply limited. These effects confirm the validity of the model. Furthermore, with that model we are able to reproduce experimental results which we have obtained with viewing targets[1]. The different spatial distribution of starting conditions generates ions with different $\int B ds$ after extraction, which also degrades the beam quality.

BASIC PRINCIPALS

General Plasma Characteristics

Due to the condition of charge neutrality for any plasma, the number of electrons n_e and the number of ions $n_{i,a}$ with charge state a can be estimated by:

$$\frac{n_e - \sum_{a=1}^{qmax} a \cdot n_{i,a}}{n_e} \ll 1 \quad (1)$$

The Debye shielding is deduced by solving Poisson's equation in a spherical coordinate system with the assumption, that there is no angular dependency[2]. This assumption is of not correct because of the magnetic field. If there would be no magnetic field, λ_D is given by:

$$\lambda_D = \sqrt{\frac{\varepsilon_0 k T_e}{n_e e^2}} = 7.43 \cdot 10^3 \sqrt{\frac{T_e [eV]}{n_e [m^{-3}]}} \quad (2)$$

where k is Boltzman's constant, T_e is the electron temperature, respectively T_i the ion temperature, e the electron charge, and ε_0 the dielectric constant. The formulation of the Debye length λ_D is valid only, if the number of particles N_D within a sphere with radius λ_D is $\gg 1$.

$$N_D = n_e \frac{4}{3} \pi \left(\frac{\varepsilon_0 k T_e}{n_e e^2} \right)^{3/2} = 1.72 \cdot 10^{12} \frac{T_e^{1.5} [eV]}{\sqrt{n_e [m^{-3}]}} \quad (3)$$

This condition is fulfilled if we assume a typical particle number of $n_e = 10^{15..18} m^{-3}$, and a Debye length in the range of μm to mm, which means that the required conditions for a plasma are satisfied. However, the Debye length within the magnetic field is not isotropic any more. Equ. 2 might be valid in the direction of the magnetic field, but not perpendicular to it.

If dynamic shielding is investigated, the plasma frequency ω_p comes into consideration. For electrons it follows:

$$\omega_p = \sqrt{\frac{n_e e^2}{m_e \varepsilon_0}} = 56.5 \sqrt{n_e [m^{-3}]} \quad (4)$$

The plasma frequency for ions with mass m_i and density $n_{i,\alpha}$ is derived by the same procedure as for electrons with mass m_e . Because the plasma frequency for ions is lower by the factor of $\sqrt{\frac{m_i}{m_e}}$, this frequency is not of importance for screening. Only electromagnetic fields with frequencies above the plasma frequency ω_p should be able to penetrate the plasma and to propagate through the plasma.

According to [3] the mean free path length of collisions between electrons is comparable to the mean free path length of collisions between ions, if electron temperature T_e and ion temperature T_i are equal: $T_e = T_i$. In that case the mean free path length can be estimated with:

$$\lambda[m] \approx 2 \cdot 10^{16} \frac{T[eV]^2}{n[m^{-3}]} \quad (5)$$

If we assume an ion temperature of 1 eV and an ion density n_i of $10^{16} m^{-3}$ this length would be 2 m. Even that this number depends on unknown quantities, it seems to be larger than the dimension of the plasma chamber. This is why collisions will not contribute to the distribution function f_α in Equ. 13.

Motion of Charged Particles within a Magnetic Field

The equation of motion for a charged particle within a magnetic field is described by the Lorentz equation:

$$m\dot{\vec{v}} = q \cdot \vec{v} \times \vec{B} \quad (6)$$

Because the force on the particle is perpendicular to \vec{B} , only the velocity perpendicular to \vec{B} is affected. It can be shown, that this creates a motion of gyration. The electron cyclotron resonance frequency ω_{ce} can be calculated by:

$$\omega_{ce} = 1.76 \cdot 10^{11} \mathbf{B}[T] \quad (7)$$

respectively for ions with atomic mass z , ω_{ci} is:

$$\omega_{ci} = 4.11 \cdot 10^9 \cdot \frac{\mathbf{B}[T]}{\sqrt{z}} \quad (8)$$

The Larmor radius for electrons $r_{L,e}$ is:

$$r_{L,e}[m] = 3.38 \cdot 10^{-6} \frac{\sqrt{T_e}[eV]}{B[T]} \quad (9)$$

respectively for ions $r_{L,i}$:

$$r_{L,i}[m] = 6.2 \cdot 10^{-3} z \frac{\sqrt{T_i}[eV]}{B[T]} \quad (10)$$

In addition to the Lorentz force another force might appear in the equation of motion.

$$m\dot{\vec{v}} = \vec{F} + q\vec{v} \times \vec{B} \quad (11)$$

If such an additional force is acting, closed circles are not possible for charged particles any more. In a mirror device, particles will be trapped if their magnetic momentum is less than the amount which would be necessary to leave the trap. Especially, if $\frac{d\vec{B}}{dt} = \frac{d\vec{E}}{dt} = 0$, the guiding center approach can be used.

$\vec{E} \times \vec{B}$ Drift If we assume the magnetic field mainly in longitudinal direction, and an ellipsoidal shape of the plasma (resulting in an electric field in radial direction), we should expect an azimuthal drift of that ellipsoid. The marks on each end of the plasma chamber could be explained with such a drift, see Fig. 1,2. Depending on the direction of the longitudinal magnetic field, the azimuthal rotation is either clock-wise or counter-clock-wise. The fact, that the observed rotation does not change its direction with increasing radius indicates that there is no change in sign of the electric field. The electric field depends on the plasma potential, which can be estimated using Bohm's sheath criterion, where the potential drop between the plasma chamber wall (on negative potential) and the plasma itself is:

$$\Phi = -T_e \ln\left(\sqrt{\frac{m_i}{2\pi m_e}}\right) \quad (12)$$

For protons, plasma potential should be in the order of $2.8 \cdot T_e$, for heavy ions up to $5.5 \cdot T_e$ [4]. For the electron temperature T_e only the cold electrons should be of importance, otherwise unrealistic high plasma potential would be estimated. The exact electron distribution over the full energy range would be required to solve that equation exactly.

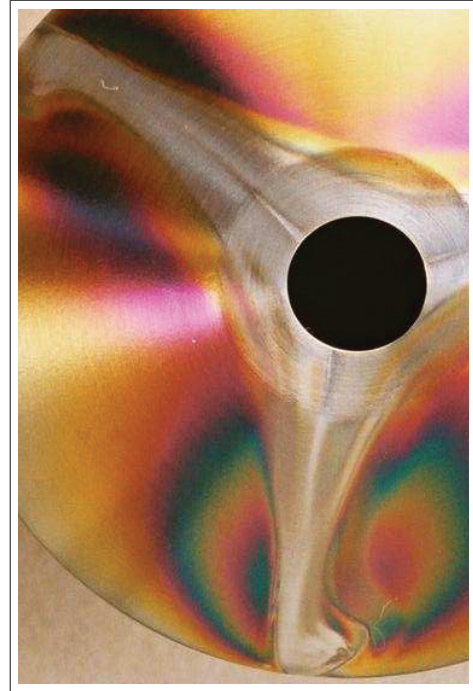


Figure 1: Plasma side of the extraction electrode showing the marks caused by the plasma. Two different traces are visible: a very thin groove, absolutely straight lined, and a more broadened structure, showing an azimuthal dependency.

Furthermore, assuming this kind of drift an explanation of the thin straight groove and the rotated erosion mark (see Fig. 1) can be given: whereas the thin groove is caused by the ions going into the loss cone at the position of the ex-

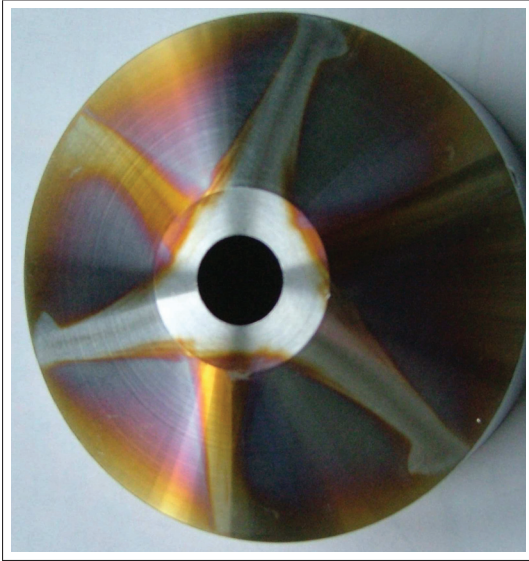


Figure 2: Extraction electrode used for ^{12}C . After some time of operation the polarity of magnetic mirror field has been reversed. The marks caused by the plasma are now orientated into the opposite azimuthal direction.

traction electrode, the larger mark is caused by the ions coming from different longitudinal positions by $\vec{E} \times \vec{B}$ drift.

Other forces causing a drift motion like diamagnetic drift, polarization drift, curvature drift, or $\nabla \vec{B}$ drift beside the electric force can be neglected.

Fluid Model

Going from the description of single particle motion to the description of fluid motion, the distribution \tilde{f}_α of the particles has to be known. The tilde indicates that the distribution function is averaged and different distribution functions for different ions, indicated by α , might exist. This distribution function might be different for electrons, ions, and for the specific charge-to-mass ratios for different ions. Of course, the distribution function will depend on the external forces as well: magnetic flux density distribution, and the rf parameter, at least for the electrons.

$$\frac{\partial \tilde{f}_\alpha}{\partial t} + \vec{v} \nabla \tilde{f}_\alpha + \frac{q}{m} (\vec{E} + \vec{v} \times \vec{B}) \nabla_v \tilde{f}_\alpha = \frac{\partial f_\alpha}{\partial t} \quad (13)$$

The homogeneous form of equ.13 is the so-called Vlasov equation. This equation is solved with an iterative method by the program KOBRA3-INP[®][5] used for simulation. The right hand side of this equation describes a collision term, negligible if the contribution of collisions is small. Note, that the left hand side contains averaged values (\tilde{f}_α) only.

Diffusion

Substituting Fick's law:

ISBN 978-3-95450-123-6

$$nu = -D \nabla n \quad (14)$$

into the continuity equation yield the diffusion equation for one specie:

$$\frac{\partial n}{\partial t} - D \nabla^2 n = 0 \quad (15)$$

where n is the number of particles, v is the velocity, and D the diffusion constant.

Because of the magnetic field the diffusion coefficient D has to be modified for charged particles, using the mean radius of gyration r_L [4], instead of using the mean free path length λ .

$$D = \frac{\pi}{8} r_L^2 v_m \quad (16)$$

According Equ.16 diffusion effects should decrease quadratically with increasing magnetic flux density. A more detailed derivation[6] shows that the diffusion constant for electrons in the direction of the magnetic field depends on density and temperature:

$$D_{\parallel e} = 1.2 \cdot 10^{22} T_e^{2.5} [eV] / n [m^{-3}] \quad (17)$$

whereas the diffusion coefficient perpendicular to the magnetic field shows a different behavior:

$$D_{\perp e} = 4 \cdot 10^{-22} \frac{n [m^{-3}]}{\sqrt{T_e [eV]} B^2 [T]}. \quad (18)$$

For ions the perpendicular diffusion is larger by $\sqrt{m_i/m_e}$, while the diffusion parallel to the magnetic field scales with $\sqrt{m_e/m_i}$.

All experimental experiences indicate that diffusion effects are small, respectively can be neglected, see Fig. 3 to 5. Otherwise the clearly separated erosion marks from unaffected regions would not be possible. It even has been found very early, that additional holes in the extraction electrode can be used to improve the pumping speed from the plasma chamber, without contributing to the extracted ion current, however, only if the orientation of the plasma electrode is correct, see Fig. 5.

EXPERIMENTAL RESULTS

There are several experimental observations, which are similar for all existing ECRIS. The pattern on the plasma chamber wall (see Fig. 3), including both end plates (see Fig. 1,2) is one of them.

On the extraction electrode a pattern can be found, which needs clarification. Two different contributions are visible: one very thin groove, absolutely straight lined in radial direction (see Fig. 1), and another wider pattern showing some azimuthal movement, depending on the radius (see Fig. 2). This movement could be interpreted as consequence of an $\vec{E} \times \vec{B}$ drift. The direction of the azimuthal

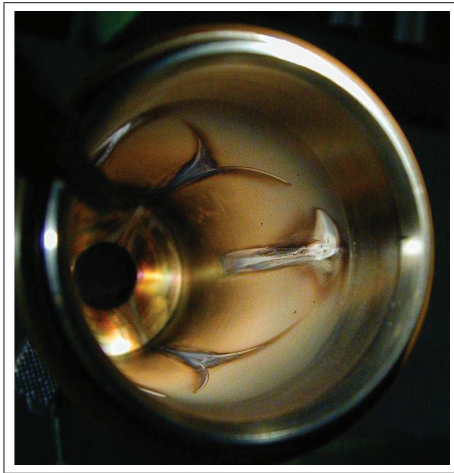


Figure 3: Plasma chamber showing the radial loss lines caused by the superposition of the magnetic mirror field and the hexapolar field.

movement can be found in both azimuthal directions, depending of course on the direction of the solenoidal magnetic field. No experimental result has been found where different directions were obtained simultaneously, indicating that the electric field would change sign.

This azimuthal movement is in addition to the one caused by the fringing field of the ion source solenoid.

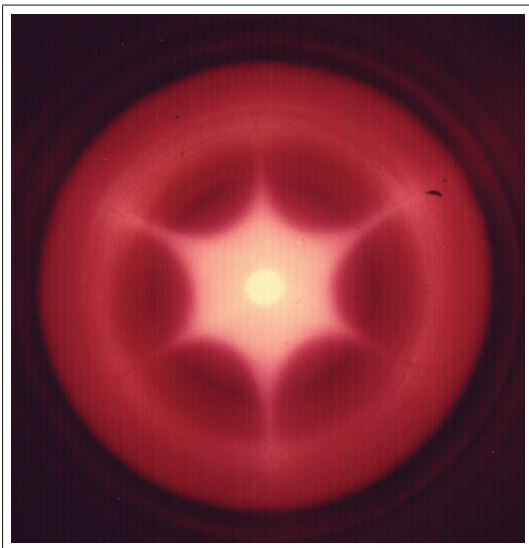


Figure 4: View into the plasma chamber with plasma. Extraction electrode has been removed for that picture [7].

The influence of different ion source parameters (gas pressure, magnetic flux density distribution, multiple frequency heating) on the local plasma density distribution is nicely demonstrated in a video produced by the ANL ECR group[8]. In that video the influence of different heating frequencies is demonstrated. Ramping individu-

ally the coils for the magnetic confinement, or ramping the gas pressure shows influence on the light, emitted from the plasma. Always a strong confinement dominates diffusion processes.



Figure 5: Extraction electrode with additional holes for pumping. No additional load for the extraction power supply caused by these additional holes has been observed (left). In case the plasma electrode is not aligned to the hexapolar pattern additional current load has been observed (right)[9].

SIMULATION

The magnetic field has been calculated using Vectorfield[®][10] software. The flux density is then imported by KOBRA3-INP[®]. Figure 6 shows magnetic field lines going through the extraction aperture at a radius of 5 mm and an azimuthal increment of 1 degree (in total 360 magnetic field lines). When the magnetic flux density along the field line is larger than the flux density within the extraction aperture, starting coordinates for the ions are generated and the color of the field line changes to red. These ions are extracted and are shown for the case of Ar³⁺ in Figure 7 and for a certain distribution of different Argon charge states in Figure 8. The theory of Self[11] can be applied along the magnetic field line, to ensure space charge compensation close to the plasma potential.

Note, that the discrete distribution in radial direction is artificial and only for better understanding of the figures. It is caused by the fact that the analyzed magnetic field lines, going through the extraction aperture, have been analyzed by circles with 1 mm radial increment in between.

It should be pointed out, that this solution shows all possible trajectories. The particle distribution f_{α} at the beginning of the trajectory is still unknown. It could be demonstrated in experiment [8],[12] that this distribution will be influenced by rf-frequency, rf-power, magnetic field distribution, and gas pressure.

For the simulation the correct magnetic fields have to be used. More information about the initial particle density distribution functions f_{α} is required, only simulations are available[13].

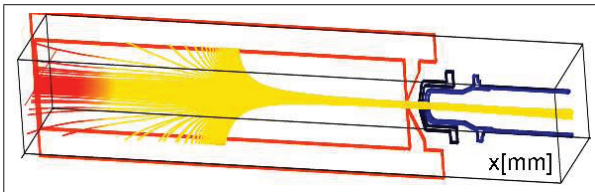


Figure 6: Magnetic field lines going through the extraction aperture on a circle of 5 mm. Depending on the azimuthal coordinate, the starting point of the field line could be located within the hexapole or at the center of the injection side.

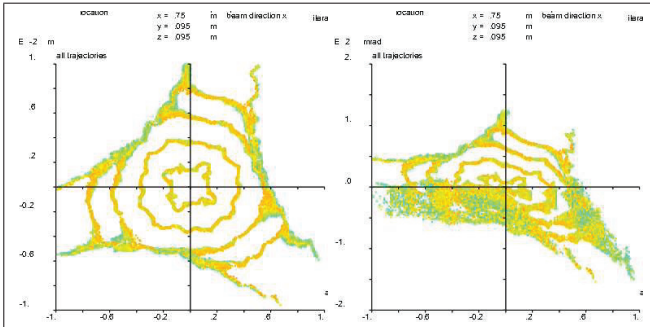


Figure 7: Real space (profile) and horizontal emittance directly behind extraction. Scale is ± 1 cm, respectively ± 200 mrad.

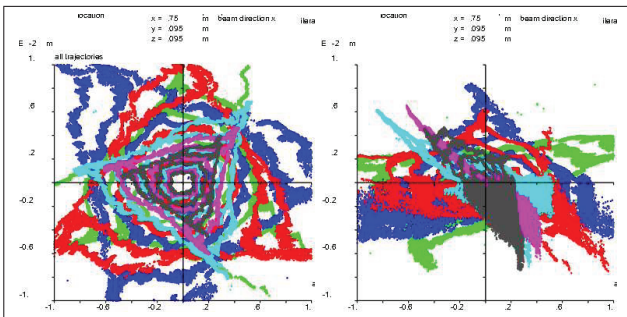


Figure 8: Real space (profile) and horizontal emittance at the same location as in Fig. 7. Blue: Ar^+ , red Ar^{2+} , green: Ar^{3+} , light blue: Ar^{4+} , magenta: Ar^{5+} , grey: Ar^{6+} . The different focal lengths of different charge states are clearly visible.

REFERENCES

- [1] P. Spädtke, K. Tinschert, R. Lang, J. Mäder, J. Roßbach, J.W. Stetson, L. Celona, RSI Vol. **79** No. 2, 02B716 (2008).
- [2] E. Debye and E. Hückel, Z. Physik **24**, 185 (1923).
- [3] Hartmut Zohm, Plasmaphysik, lecture notes, LMU Munich, 2010, in German.
- [4] M.A. Lieberman, A.J. Lichtenberg, Principals of Plasma Discharges and Material Processing, John Wiley & Sons, Inc., (1994).
- [5] INP, Junkernstr. 99, 65205 Wiesbaden, Germany.
- [6] U. Stroth, Plasmaphysik, ISBN 978-3-8348-1615-3.
- [7] Fred W. Meyer (ORNL), private communication.
- [8] Video on YouTube produced by Mike Bentrain ATLAS, Argonne National Lab, (2007).
- [9] R. Geller, D. Hitz, private communication.
- [10] Vectorfield Software, Cobham Technical Services, Brook Road, Wimborne, Dorset, UK.
- [11] S.A. Self, Phys. Fluids **6**, p. 1762, 1963.
- [12] F. Maimone, L. Celona, R. Lang, J. Mäder, J. Roßbach, P. Spädtke, and K. Tinschert, Rev. Sci. Instrum. **82**, 123302 (2011).
- [13] D. Mascali, S. Gammino, L. Celona, and G. Ciavola, Rev. Sci. Instrum. **83**, 02A336 (2012).